

Recyclable TPA-Modified MIL-88-Supported Ionic Pt as a Highly Efficient Catalyst for Alkene Hydrosilylation

Muhua Chen,* Peng Chen, Zhen Ji, Min Yu, Jihuai Tan, Bo Fu, and Xinbao Zhu

Cite This: *ACS Omega* 2023, 8, 13323–13331

Read Online

ACCESS |

Metrics & More

Article Recommendations

Supporting Information

ABSTRACT: The hydrosilylation reaction driven by a homogeneous catalyst has been widely used in the industrial synthesis of functionalized silicone compounds. However, the homogeneous catalyst for hydrosilylation has the shortcomings of nonrecyclability, undesirable side reactions, and high cost. In this work, a highly efficient heterogeneous catalyst was prepared by loading Pt ions on MIL-88 modified with trimethoxy[3-(phenylamino)propyl]silane. In comparison with previous research studies, the resulting catalyst can exhibit high catalytic activity and excellent stability during the hydrosilylation reaction, which was attributed to the presence of a pyrrolic nitrogen structure between TPA-MIL-88 and the Pt ion. Besides them, 1.2%Pt/TPA-MIL-88 showed the highest catalytic activity and can be reused five times without significant deactivation. Importantly, 1.2%Pt/TPA-MIL-88 also achieved satisfactory results when it was used to catalyze the hydrosilylation reaction for other olefins, implying great potential for application in the silicone industry.



1. INTRODUCTION

The hydrosilylation reaction is one of the most commonly used reactions for the industrial preparation of functionalized silicone polymers,^{1–5} especially for the synthesis of silicon monomers containing various functional groups, which has been widely used in the fields of coatings,⁶ medical devices,⁷ flame retardants,⁸ and three-dimensional (3D) printing.⁹ For decades, the catalysts for hydrosilylation have been homogeneous, which mainly consist of organic ligands and noble metals, such as Pt, Ru, Pd, and Rh.^{10,11} Among them, Pt-based Speier (isopropanol solution of chloroplatinic acid hydrate) and Karstedt (zero-valent platinum complex) catalysts are the most widely used in industry.^{12,13} However, those homogeneous catalysts are difficult to be recovered, which inevitably results in the high production cost and price.

To address the issue, introducing homogeneous Pt compounds onto the surface of different supports with a large specific surface has received extensive attention. For example, Cui et al. prepared a Pt single-atom Al₂O₃ nanorod-loaded catalyst Pt/NR-Al₂O₃-IP by an impregnation method, which showed a high catalytic selectivity and a wide catalytic range by catalytic reactions with different olefins, tertiary silanes, and polysiloxanes. The catalytic yield still reached more than 92% after it was reused six times.¹⁴ Xie et al. prepared a Pt/CS-SiO₂ catalyst by modifying SiO₂ with chitosan and loading it with platinum. The catalyst catalyzed the reaction of propylene glycol polyether with heptamethyltrisiloxane and obtained a β -addition product in 94% yield.¹⁵ Li et al. prepared a new SiO₂-loaded platinum catalyst SiO₂-ethylenediaminetetraacetic acid (EDTA)-Pt by grafting ethylenediaminetetra-

acetic acid (EDTA) onto a silica carrier containing amino-propyltriethoxysilane in the addition reaction of 1-hexene and methylchlorosilane. The resulting catalyst exhibited excellent selectivity; the catalytic yields were still over 80% after it was reused for five times.¹⁶ Despite the good catalytic efficiency of the above heterogeneous catalysts, most of them still suffer from the disadvantages such as high platinum load and easy leaching of active species. Thus, it is still a challenge to develop a recyclable catalyst with good catalytic performance by combining the advantages of homogeneous and heterogeneous catalysts.^{17,18}

Metal-organic frameworks (MOFs) have been widely applied in optics,¹⁹ sensors,²⁰ gas adsorption and separation,²¹ gas storage,²² catalysis, and drug delivery due to their adjustable regular network structures and pore channels.^{23–25} MOFs are novel inorganic-organic porous coordination compounds formed by coordination bonds between metal cluster ions and aromatic ligands or ammonia heterocyclic compounds.^{26,27} Among them, MIL-88(Fe) with good thermal stability is a fusiform crystalline metal-organic backbone formed by iron ions linked to terephthalic acid with multiple unsaturated metal sites.²⁸ Rahmani et al. synthesized MIL-

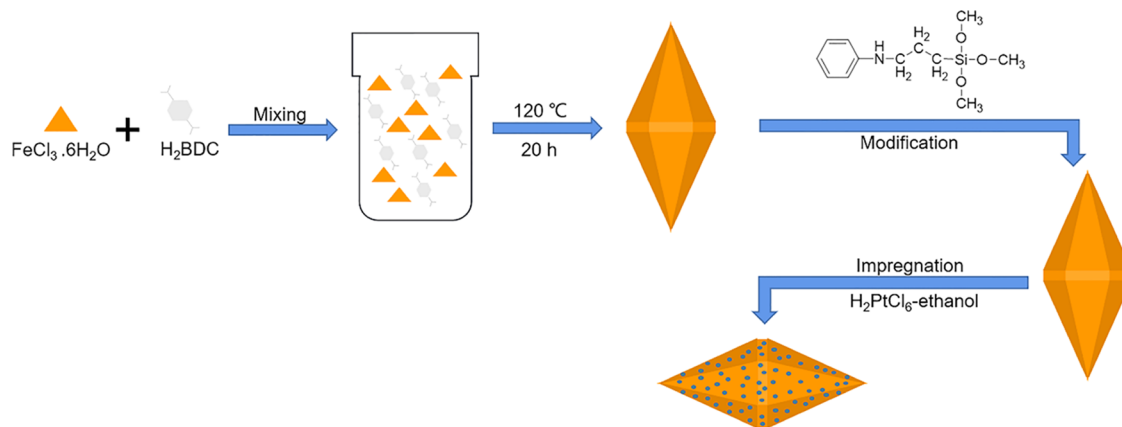
Received: February 2, 2023

Accepted: March 21, 2023

Published: April 3, 2023



Scheme 1. Flow Chart of Catalyst Preparation



101(Fe) and MIL-88(Fe) by a solvothermal method and used the synthesized materials to catalyze the alkylation of benzene with ethanol. The results showed that the new catalysts can be used at low temperature and low pressure.²⁹ Jintu et al. prepared a microporous MIL-88-NH₂ metal-organic backbone using a simple template-guided method and a structure-guiding agent (cetyltrimethylammonium bromide) to synthesize HP-MIL-88-NH₂ catalysts.³⁰ It exhibited an excellent catalytic performance for the cycloaddition reaction of CO₂ and epoxide at atmospheric pressure and low reaction temperature. Xie et al. successfully loaded platinum on 2-aminoethanethiol (AET)-modified MIL-101 using an impregnation method, and the obtained catalyst was used to catalyze the hydrosilylation reaction of olefins.³¹ After reusing five times, its conversion still reached to 84%. Compared with 2-aminoethanethiol, silane coupling agents have more amino and hydrolytic hydroxyl groups, which can bind the noble metal ions more firmly, delivering good catalytic properties.^{32,33} Shimazaki et al. prepared a PtRu/C catalyst by a pH-controlled one-pot process with a silane coupling agent. The results suggested that the existence of (3-aminopropyl) trimethoxysilane (APS) coating not only promoted the dispersive adsorption of PtRu nanoparticles but also improved the durability of the catalyst in an acidic environment.³⁴ Zai et al. synthesized a heterogeneous pseudo-single-atom Pt catalyst with high activity and recyclability in the hydrosilylation of allyl-terminated polyether with polymethylhydrosiloxane. The functionalization of the SiO₂ shell with silane coupling agents containing vinyl groups allows stabilizing Pt on the SiO₂ surface through complexation. The Pt/vinyl/SiO₂/Fe₃O₄ catalyst can be reused up to four reaction cycles.³⁵

In this work, recyclable 1.2%Pt/trimethoxy[3-(phenylamino)propyl]silane (TPA)-MIL-88 as a highly efficient catalyst for alkene hydrosilylation was first prepared through the following processes: (i) MIL-88 was modified with the modifier TPA to synthesize the TPA-MIL-88; (ii) the platinum species (chloroplatinic acid-ethanol solution) was loaded on TPA-MIL-88 by impregnation to form the novel catalyst XPt/TPA-MIL-88 ($X = 0.8, 1.2$ and 1.6%). The hydrosilylation reaction results showed that the 1.2%Pt/TPA-MIL-88 catalyst possessed excellent catalytic activity and good stability. The structure-performance relationship of the 1.2%Pt/TPA-MIL-88 catalyst in the catalytic hydrosilylation reaction was discussed in detail. Moreover, the hydrosilylation with various olefins of the 1.2%Pt/TPA-MIL-88 catalyst was further studied for potential industrial application.

2. EXPERIMENTS

2.1. Reagents. All chemical reagents are purchased without further purification. Chloroplatinic acid hexahydrate ($\text{H}_2\text{PtCl}_6 \cdot 6\text{H}_2\text{O}$), *N,N*-dimethylformamide (DMF), heptamethyltrisiloxane (HET), trimethoxy[3-(phenylamino)propyl]silane (TPA), and 3-mercaptopropyltriethoxysilane were purchased from Shanghai Aladdin Biochemical Technology.

Ethanol and toluene were purchased from Nanjing Chemical Reagent Co., Ltd. Deionized water was obtained from an electric water distiller produced by Shaoxing Supo Instrument Co., Ltd. Terephthalic acid (H_2BDC), iron chloride hexahydrate ($\text{FeCl}_3 \cdot 6\text{H}_2\text{O}$), allyl glycidyl ether (AGE), 1-hexadecene, styrene, 1-dodecene, and 1-tetradecene were purchased from Shanghai Maclin Biochemical Technology Co., Ltd.

2.2. Catalyst Preparation. **2.2.1. Synthesis of MIL-88.** MIL-88 was synthesized according to a method described in the published literature with minor improvements.²⁸ 8 mmol $\text{FeCl}_3 \cdot 6\text{H}_2\text{O}$ was dissolved in 50 mL of DMF and stirred with magnetic force for 1 h, and then 8 mmol H_2BDC was added for another 3 h. Then, ultrasonic treatment was carried out for 30 min, and magnetic stirring was done for 30 min. The obtained mixture was placed in a 100 mL Teflon-lined stainless steel autoclave and heated for 20 h at $120\text{ }^\circ\text{C}$. After cooling down to room temperature, the organic solvent was removed by centrifugation and the precipitate was washed with deionized water and anhydrous ethanol three times and finally dried in vacuum at $80\text{ }^\circ\text{C}$ overnight.

2.2.2. Synthesis of TPA-MIL-88. The prepared MIL-88 was dehydrated at $150\text{ }^\circ\text{C}$ in a vacuum oven for 12 h. Then, 0.5 g of dehydrated MIL-88 was dispersed in 30 mL of anhydrous toluene. 1.5 mmol TPA was added, and the mixture was stirred and refluxed for 12 h at $110\text{ }^\circ\text{C}$. The solid product was recycled by filtration, washed with deionized water and anhydrous ethanol three times, and then dried under vacuum at $80\text{ }^\circ\text{C}$ overnight.

2.2.3. Synthesis of XPt/TPA-MIL-88 ($X = 0.8, 1.2, 1.6\%$). 0.5 g of vacuum-dried TPA-MIL-88 was dispersed in 30 mL of anhydrous ethanol, and the required amount of H_2PtCl_6 -ethanol solution (0.0064 g/g) was added to the mixture and stirred at $80\text{ }^\circ\text{C}$ under a continuous nitrogen flow for 10 h. After cooling to room temperature, the product was washed with ethanol several times. Finally, the product was dried at $80\text{ }^\circ\text{C}$ for 24 h. For comparison, 1.2%Pt/MIL-88 catalysts were prepared by the same method described above. The preparation process is shown in Scheme 1.

Table 1. Hydrosilylation Conversion of HTE under Different Reaction Conditions

entry	catalyst	catalyst amount ^a (wt %)	temperature (°C)	AGE (mol)	conversion (%)
1	0.8%Pt/TPA-MIL-88	1.0	100	0.0396	76.37
2	1.2%Pt/TPA-MIL-88	1.0	100	0.0396	90.42
3	1.6%Pt/TPA-MIL-88	1.0	100	0.0396	90.63
4	1.2%Pt/TPA-MIL-88	1.0	90	0.0396	84.93
5	1.2%Pt/TPA-MIL-88	1.0	110	0.0396	91.68
6	1.2%Pt/TPA-MIL-88	1.0	100	0.0360	86.77
7	1.2%Pt/TPA-MIL-88	1.0	100	0.0432	91.34
8	1.2%Pt/TPA-MIL-88	0.4	100	0.0396	78.49
9	1.2%Pt/TPA-MIL-88	0.8	100	0.0396	88.47
10	1.2%Pt/TPA-MIL-88	1.2	100	0.0396	91.15
11	MIL-88	1.0	100	0.0396	1.57
12	TPA-MIL-88	1.0	100	0.0396	1.54

^aCatalyst amount: the mass ratio of catalyst to reactants.

2.3. Characterization. Powder X-ray diffraction (XRD) analyses were carried out on a Rigaku Ultima IV system. Cu K α was used as a radiation at a current of 40 mA and voltage of 40 kV. The 2 θ angles were scanned from 3 to 30 at 10°·min⁻¹.

The functional groups, chemical structures, and bonding characteristics of the prepared materials were analyzed on a Thermo Nicolet-6700 Fourier transform infrared (FT-IR) spectrometer. The samples for FT-IR characterization were prepared by the KBr compression method: 0.1 mg of the sample to be tested was mixed with 200 mg of chemically pure KBr, finely ground, and then pressed, with a wave number range of 500–4000 cm⁻¹. Nitrogen adsorption–desorption isotherms were performed on a BSD-PM2 instrument at –196 °C. Before nitrogen physisorption measurement, the species were degassed under vacuum at 100 °C for 12 h. The pore volume desorption of the resulting catalyst was evaluated using the Barrett–Joyner–Halenda (BJH) method. The micro-morphology and particle size of the materials were characterized using a Regulus 8100 field emission scanning electron microscope. The energy-dispersive spectrometry (EDS) mapping test was also performed using the scanning electron microscope to determine the elemental composition and spatial distribution in the samples. The samples are fixed on a sample stage and gold-sprayed.

Transmission electron microscopy (TEM) analysis was performed on a JEM-1400 (Japan Electronics Co.). Prior to test, the samples were added to the ethanol solvent with an ultrasonic dispersion for 30 min and deposited on carbon-coated copper grids. X-ray photoelectron spectra (XPS) were recorded on an AXIS UltraDLD (U.K.) with an Al K α (X-ray) lamphouse. Binding energies of C 1s at 284.8 eV were used as a reference. Actual Pt loading of catalytic materials was determined using inductively coupled plasma (ICP) analysis equipped with an Agilent model ICP-OES730.

2.4. Catalytic Performance Evaluation. The hydrosilylation reaction was carried out as follows: the catalyst (XPt/TPA-MIL-88 or 1.2%Pt/MIL-88) and different amounts of allyl glycidyl ether were added to a 50 mL three-neck flask and stirred at 80 °C for 10 min. Then, 0.036 mol of heptamethyltrisiloxane was added slowly dropwise and the reaction mixture was heated to a preset temperature and kept for some time. After reaction, the product and catalyst were separated by centrifugation (8000 rpm, 8 min, 25 °C). The hydrosilylation reaction for other olefins were carried out in the same way.

The liquid products were analyzed via a GC-2010 gas chromatograph (GC-2010, Shimadzu), equipped with a flame ionization detector (FID) and a Rtx-5 capillary column (30 m × 0.25 mm × 0.25 μ m). The conversion of heptamethyltrisiloxane was calculated using the following equation

$$\text{conversion (\%)} = (M_1 - M_2)/M_1 \times 100\%$$

where M_1 is the initial addition of HTE (g) and M_2 is the mass of HTE after reaction (g).

The hydrogen spectra of the products were determined on a BRUKER AV600 (Switzerland) NMR instrument using deuterated chloroform (CDCl₃) as a solvent. For the recycling experiment, the catalyst was washed with anhydrous ethanol and dried at 80 °C for 12 h under vacuum. Then, the dried catalyst was reused in the next run.

3. RESULTS AND DISCUSSION

3.1. Catalytic Hydrosilylation of Alkenes. Numerous studies have shown that platinum is an effective catalyst for olefin hydrogenation reactions.^{36,37} Herein, the abovementioned catalysts are used to catalyze the hydrosilylation reaction with HTE and AGE as substrates. Effects of different reaction conditions on the catalytic activity of XPt/TPA-MIL-88 were investigated. The catalytic results are presented in Table 1. Under the same catalytic conditions, the 1.2%Pt/TPA-MIL-88 catalyst outperformed the 0.8%Pt/TPA-MIL-88 and basically reached the same level of 1.6%Pt/TPA-MIL-88 catalysts (Table 1, entries 1–3). The effect of reaction temperature on the catalytic activity was examined using the preferred sample 1.2%Pt/TPA-MIL-88. An increase in temperature from 90 to 100 °C promoted the HTE conversion by 5.49%; when the temperature was reacted at 110 °C, there was a slight enhancement in HTE conversion (growth margin: 1.26%), but the product after the reaction changed from colorless to yellow. It is believed that the color change caused by the increase inside reactions was associated with the high temperature. Therefore, the optimal catalytic temperature for the hydrosilylation reaction is set at 100 °C. Based on the above conditions, the effect of different molar ratios of reaction substrates (AGE/HTE) on the conversion of HTE is investigated. The conversion is only 86.7% at a molar ratio of 1:1, and the conversion is significantly higher and closer at both molar ratios of 1.1:1 and 1.2:1 (Table 1, entries 6, 2, 7). The optimum molar ratio of 1.1:1 is chosen considering the practical application.

Then, the effect of catalyst amount on the hydrosilylation reaction was studied. Compared to 0.8 wt % dose (HTE conversion: 88.47%), HTE conversion of 1.0 and 1.2 wt % dose increased by 1.95 and 2.68%, respectively (Table 1, entries 9, 2, 10). This is due to the initial saturation state of the catalytic center required for the unit substrate reached at a dose of 0.8 wt %. Based on the above results, a dose of 1.0 wt % is set as the optimal catalyst dose for the reaction.

3.2. Structural Properties. As shown in Figure 1, the main peaks observed in XRD patterns are in good agreement

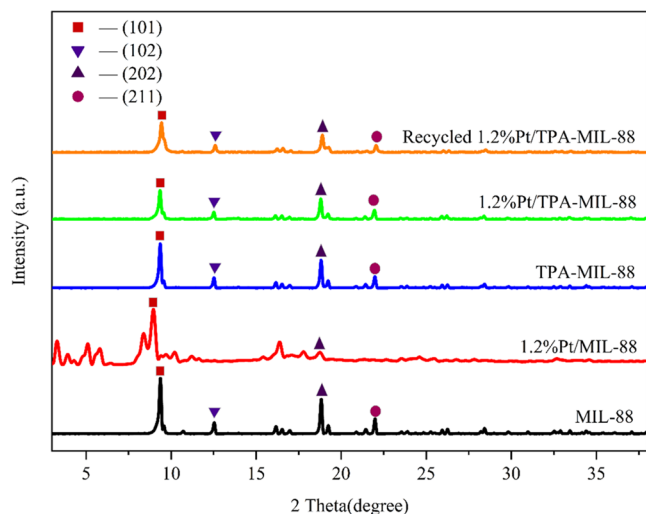


Figure 1. XRD patterns of synthesized precursors and catalyst samples.

with previous reports,^{38,39} corresponding to (101), (102), (202), and (211) crystallographic planes, which indicates the good crystallinity of the synthesized MIL-88. No peaks attributed to Pt species are observed for all samples. When Pt was loaded on unmodified MIL-88, the XRD pattern of 1.2%Pt/MIL-88 showed a significant shift in the peak positions and a widening of peak half-width. This suggests that the acidic environment of the Pt source (chloroplatinic acid) may be detrimental to the metal–organic skeleton.⁴⁰ After grafting TPA on the metal–organic backbone of MIL-88 and adding Pt, none of the peak positions change significantly in 1.2%Pt/TPA-MIL-88, indicating that the crystal structure of MIL-88 can be well maintained during the grafting and loading of Pt. Namely, the modifier can be confirmed to have a positive effect on stabilizing the structure of the support during the loading process.

The synthesized precursors and catalyst samples were investigated by FT-IR spectroscopy. The general features of FT-IR spectra (Figure 2) for these samples are almost identical to those of reported MIL-88(Fe).^{41,42} It can be found that the stretching vibration peak belonging to C=O at 1600 cm^{-1} of 1.2%Pt/MIL-88, which comes from an organic ligand, is significantly weakened comparing with MIL-88. As consistent with the XRD analyses, it can be confirmed that the loading of Pt on unmodified MIL-88 causes framework collapse of MIL-88. Comparison of the spectra reveals several new characteristic peaks for TPA-MIL-88 and 1.2%Pt/TPA-MIL-88 due to grafting of TPA. A weak peak at 2940 cm^{-1} belongs to the asymmetric stretching vibration of $-\text{CH}_2-\text{CH}_2-$, and sharp peaks at 1120 and 690 cm^{-1} are assigned to the stretching vibration of Si–O–C and Si–C bonds, respectively.⁴³ The

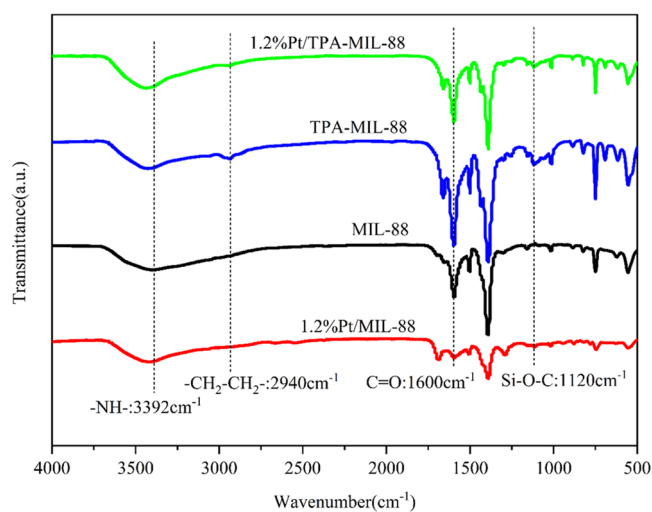


Figure 2. FT-IR spectra of synthesized precursors and catalyst samples.

appearance of these characteristic peaks indicates that TPA successfully modified the MIL-88. Furthermore, the FT-IR spectrum of TPA (Figure S1) shows the original stretching vibration peak of Si–O–C at 1074 cm^{-1} , while the peak migrates to a higher wave number after grafting and loading Pt. It demonstrates that the self-condensation of silicohydroxy is formed by the methoxyl end of the silane with the hydroxyl group on the support.⁴⁴ There is no observable stretching vibration peak of the $-\text{NH}-$ group (3392 cm^{-1}) both in FT-IR spectra of TPA-MIL-88 and 1.2%Pt/TPA-MIL-88, which may be attributed to the broad strong intensity of hydroxyl groups enwrapping on catalyst samples.

The microscopic structures of the prepared materials were detected by scanning electron microscopy (SEM) and transmission electron microscopy (TEM). Figure 3a shows a typical low-magnification SEM image of the bare MIL-88. MIL-88 is composed of a large number of spindle-like structures with lengths of 0.5–0.7 μm . After direct loading of Pt on the support MIL-88, the obtained 1.2%Pt/MIL-88 shows obvious crystalline disruption and the particle size is no longer uniform (Figure 3b). After grafting TPA onto MIL-88 (TPA-MIL-88, Figure 3c) and loading Pt (1.2%Pt/TPA-MIL-88, Figure 3d), the crystalline morphology does not change significantly and crystal particle size remains essentially the same as that of MIL-88. It can be speculated that a protective layer was formed by condensation of the OH group during TPA grafting to MIL-88.^{45,46} According to EDS mapping (Figure 3e), it is confirmed that the loaded Pt species was uniformly distributed on the catalyst. A very small amount of nanoparticles of Pt species can also be observed at the edge of the crystalline support in the TEM image (Figure 3f).

The surface area and porous structure of the samples were analyzed using a N_2 adsorption–desorption instrument, and the results are shown in Figure 4 and Table 2. Comparing with MIL-88, the specific surface of 1.2%Pt/MIL-88 decreased by 39.5 $\text{m}^2\cdot\text{g}^{-1}$ and the pore size increased conversely, revealing a partial framework collapse of the unprotected MIL-88 during the loading of Pt. After modification with TPA, the specific surface reduced to 92 $\text{m}^2\cdot\text{g}^{-1}$, and the pore volume and diameter are decreased to 0.13 $\text{m}^3\cdot\text{g}^{-1}$ and 6.4 nm, respectively. This remains essentially the same as 1.2%Pt/TPA-MIL-88 after further loading with chloroplatinic acid because the modifier

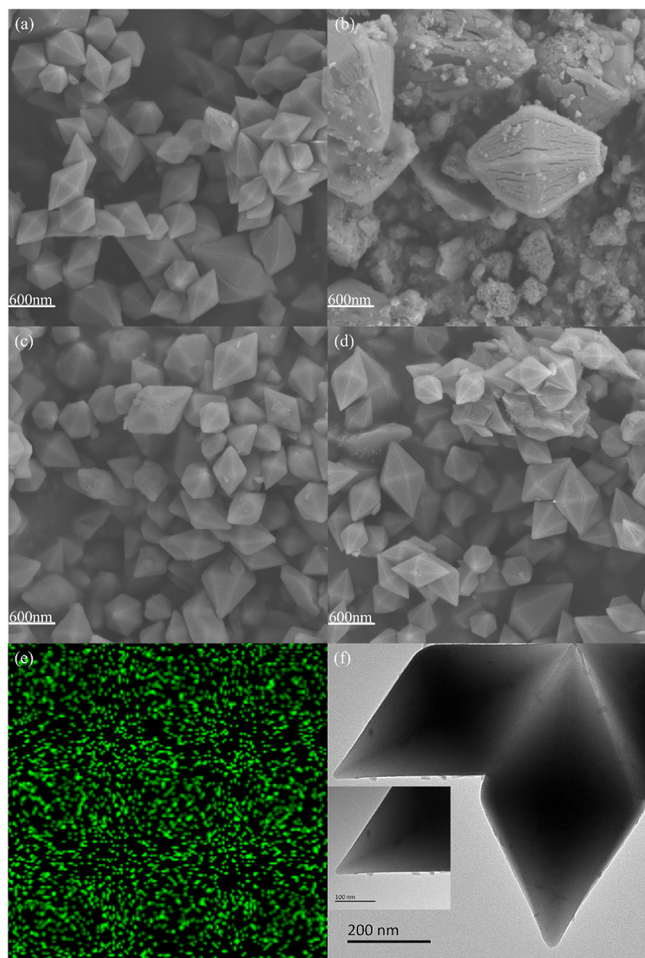


Figure 3. SEM images of MIL-88 (a), 1.2%Pt/MIL-88 (b), TPA-MIL-88 (c), and 1.2%Pt/TPA-MIL-88 (d); EDS mapping spectra (e); and TEM images (f) of 1.2%Pt/TPA-MIL-88.

molecules occupy a finite volume, which can partially obstruct the pores. The above analysis revealed that the crystal structure of MIL-88 can be protected by the TPA modification treatment, which was consistent with the analysis results of previous characterization.

X-ray photoelectron spectroscopy (XPS) measurements were carried out to elucidate the surface composition and chemical states of various samples. As shown in Figure S2, the presence of N and Si elements in the XPS spectra of TPA-

Table 2. Surface and Pore Structure of the Catalysts

samples	S_{BET} (m^2g^{-1})	pore volume (cm^3g^{-1})	average pore diameter (nm)
MIL-88	157.7	0.262	7.1
1.2%Pt/MIL-88	118.2	0.251	10.1
TPA-MIL-88	92.7	0.129	6.4
1.2%Pt/TPA-MIL-88	79.2	0.119	6.3

MIL-88 indicates that MIL-88 was modified by TPA successfully. The XPS spectrum (Figure 5a) of TPA-MIL-88 displays that the binding energy of N 1s is 399.3 eV, which demonstrates the formation of pyridine nitrogen.⁴⁷ The N 1s XPS spectrum of 1.2%Pt/TPA-MIL-88 in Figure 5b shows a binding energy of 400.2 eV, which identifies the formation of pyrrolic nitrogen after Pt loading. The results indicate that the coordination environment of Pt should be ascribed to Pt–N (pyrrolic) rather than Pt–N (pyridine) coordination.⁴⁸

As shown in Figure 5c, to determine the different chemical states of Pt species, the Pt 4f XPS spectrum of 1.2%Pt/TPA-MIL-88 were fitted for two low-frequency bands (Pt 4f_{7/2}) and high-frequency bands (Pt 4f_{5/2}) of Pt⁴⁺ and Pt²⁺. The binding energies of Pt²⁺ are 72.5 and 75.6 eV, and those of Pt⁴⁺ are 75.0 and 78.5 eV, suggesting that the Pt species of 1.2%Pt/TPA-MIL-88 is ionic. Because of promoting the electron transfer by pyrrolic-N, the binding energy of Pt in 1.2%Pt/TPA-MIL-88 is negatively shifted, which demonstrates the presence of the interaction between the Pt ion and pyrrolic-N.^{49,50} Compared with the metallic platinum catalyst, since the positron structure of Pt is generated prior to the catalytic reaction, it is contributed to an efficient reaction process with a short induction period in terms of the reaction mechanism and kinetics.⁵¹

The reusability and stability of a heterogeneous catalyst is important for industrial applications. The catalyst of the present work can be collected by a simple centrifugal separation operation, followed by several washes with ethanol and then vacuum-drying for cyclic testing. As shown in Figure 6, the HTE conversion of the unmodified 1.2%Pt/MIL-88 decreases by 15.18% in the second cycle and even by 62.10% in the third cycle. However, the TPA-grafted catalyst (1.2%Pt/TPA-MIL-88) has a very stable catalytic performance after a series of consecutive runs that the HTE conversion can be maintained at about 86% after five cycles. The slight decrease in HTE conversion of 1.2%Pt/TPA-MIL-88 can be attributed to the inevitable mass loss of the catalyst during the recycling process.

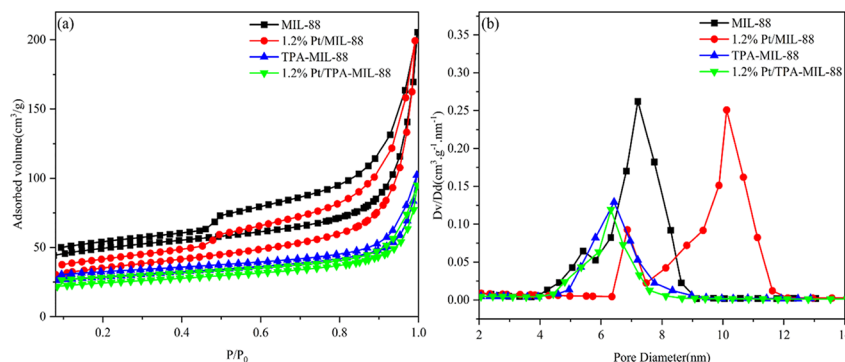


Figure 4. N₂ adsorption/desorption isotherms (a) and DFT pore size distributions (b) of MIL-88, 1.2%Pt/MIL-88, TPA-MIL-88, and 1.2%Pt/TPA-MIL-88.

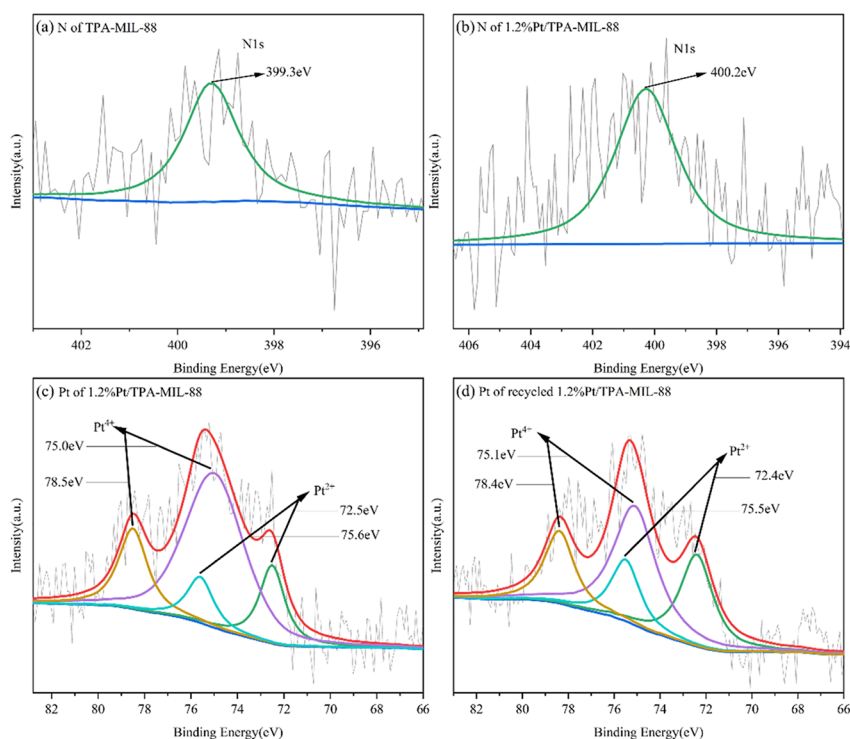


Figure 5. High-resolution N 1s XPS spectra of TPA-MIL-88 (a) and 1.2%Pt/TPA-MIL-88 (b); high-resolution Pt 4f XPS spectra of 1.2%Pt/TPA-MIL-88 (c) and recycled 1.2%Pt/TPA-MIL-88 (d).

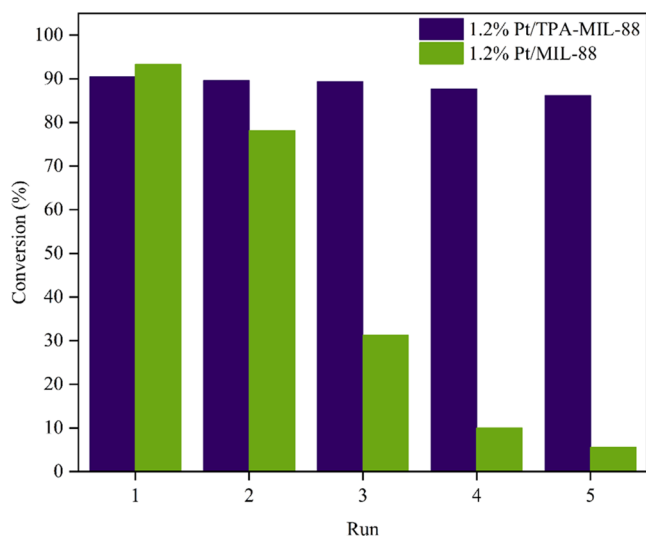


Figure 6. Reusability of 1.2%Pt/TPA-MIL-88 and 1.2%Pt/MIL-88 in the catalytic hydrosilylation.

In addition, the recycled catalysts were characterized by XRD, ICP, and XPS. The XRD analysis (Figure 1) shows that the crystallinity of the recyclable catalyst is essentially the same as that of the initial one. As shown in Table 3, the ICP test results display that the Pt loading amount of recycled 1.2%Pt/TPA-MIL-88 is 1.03 wt %, which is slightly lower than that of pristine 1.2%Pt/TPA-MIL-88 (1.23 wt %). By comparison, the Pt loading amount in unmodified 1.2%Pt/MIL-88 appears to decrease significantly (from 1.25 to 0.59 wt %). These results indicate that the Pt species in 1.2%Pt/TPA-MIL-88 with the modification of TPA can be more stable, which is attributed to the chelating effect of the pyrrolic nitrogen structure formed during the Pt loading process.⁴⁸ XPS (Figure 5d) analysis of

Table 3. Theoretical and Actual Loading Amounts of Pt in Various Catalysts

catalysts	theoretical loading (wt %)	actual loading (wt %)
1.2%Pt/TPA-MIL-88	1.2	1.23
recycled 1.2%Pt/TPA-MIL-88	1.2	1.03
1.2%Pt/MIL-88	1.2	1.25
recycled 1.2%Pt/MIL-88	1.2	0.59

the recycled catalyst shows that Pt species can remain positively charged after several cycles.

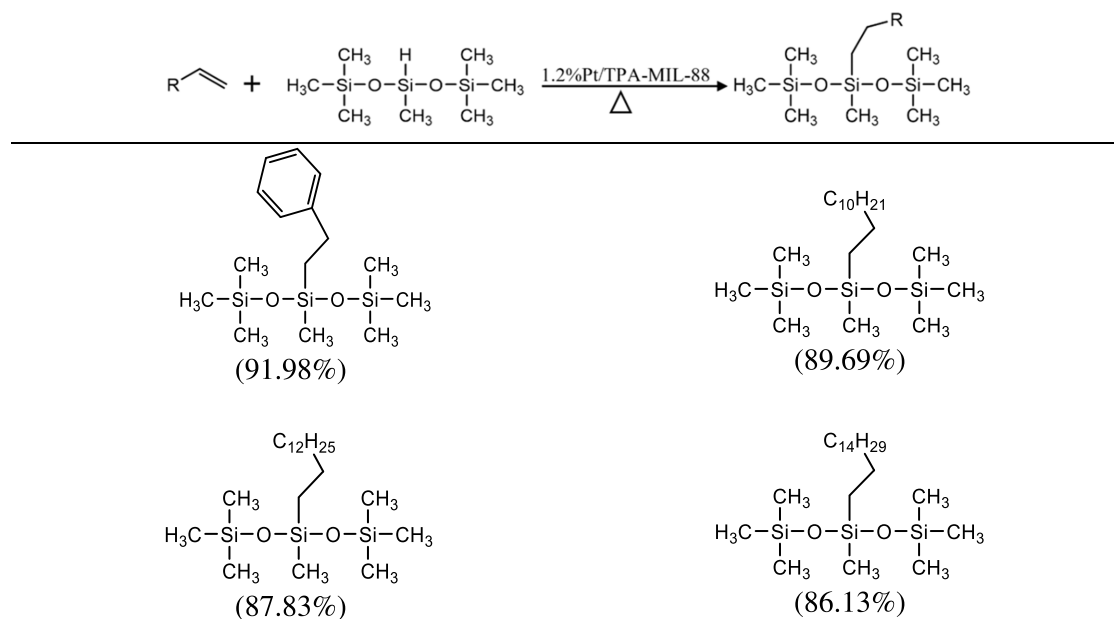
3.3. Catalytic Hydrosilylation of Different Olefins.

Furthermore, the hydrosilylation reactions of different olefins are performed to investigate the versatility of 1.2%Pt/TPA-MIL-88. As shown in Table 4, the conversion of the silane reaches 91.98% in the hydrosilylation reactions of styrene. In the hydrosilylation reactions of 1-dodecene, 1-tetradecene, and 1-hexadecene, the conversions of silane exceed more than 86%. Obviously, the catalytic results are satisfactory, although the conversion varied with the growth of the olefin molecular chain.

4. CONCLUSIONS

In summary, a homogeneous catalyst 1.2%Pt/TPA-MIL-88 was facilely prepared. After modification of MIL-88 with TPA, the endpoint of the silane modifier was connected with the support by self-condensation of the OH group to enhance the stability of TPA-MIL-88. During the loading process, owing to the imino group of TPA, Pt species was immobilized by stable Pt–N (pyrrolic) coordination and well dispersed on TPA-MIL-88. Additionally, the 1.2%Pt/TPA-MIL-88 catalyst is liable to be recycled by a simple centrifugal separation. Therefore, 1.2%Pt/TPA-MIL-88 has excellent catalytic properties, and the conversion of silane reached 90.42% and remained

Table 4. Hydrosilylation of Various Olefins and HTE by 1.2%Pt/TPA-MIL-88



above 86% after five cycles of the catalyst. These results demonstrate that 1.2%Pt/TPA-MIL-88 has great potential in the industrial production of organosilicon compounds.

■ ASSOCIATED CONTENT

SI Supporting Information

The Supporting Information is available free of charge at <https://pubs.acs.org/doi/10.1021/acsomega.3c00693>.

FT-IR spectra of TPA; XPS survey spectra of TPA-MIL-88 and 1.2%Pt/TPA-MIL-88 (a), high-resolution Fe 2p spectra of TPA-MIL-88 (b), high-resolution Fe 2p spectra of 1.2%Pt/TPA-MIL-88 (c), high-resolution Si 2p spectra of TPA-MIL-88 (d), and high-resolution Si 2p spectra of 1.2%Pt/TPA-MIL-88 (e); standard curve data for heptamethyltrisiloxane; standard curve for heptamethyltrisiloxane; ¹H NMR data of products (compound a/d/c/d/e); TGA curves of 1.2%Pt/TPA-MIL-88 and 1.2%Pt/MIL-88; and particle size distribution of MIL-88 (PDF)

■ AUTHOR INFORMATION

Corresponding Author

Muhua Chen – Jiangsu Co-Innovation Center of Efficient Processing and Utilization of Forest Resources, Jiangsu Provincial Key Lab for the Chemistry and Utilization of Agro-forest Biomass, College of Chemical Engineering, Nanjing Forestry University, Nanjing 210037, China; orcid.org/0000-0002-8383-5358; Email: simonzrh@163.com

Authors

Peng Chen – Jiangsu Co-Innovation Center of Efficient Processing and Utilization of Forest Resources, Jiangsu Provincial Key Lab for the Chemistry and Utilization of Agro-forest Biomass, College of Chemical Engineering, Nanjing Forestry University, Nanjing 210037, China

Zhen Ji – Jiangsu Co-Innovation Center of Efficient Processing and Utilization of Forest Resources, Jiangsu Provincial Key

Lab for the Chemistry and Utilization of Agro-forest Biomass, College of Chemical Engineering, Nanjing Forestry University, Nanjing 210037, China

Min Yu – Jiangsu Co-Innovation Center of Efficient Processing and Utilization of Forest Resources, Jiangsu Provincial Key Lab for the Chemistry and Utilization of Agro-forest Biomass, College of Chemical Engineering, Nanjing Forestry University, Nanjing 210037, China

Jihuai Tan – Jiangsu Co-Innovation Center of Efficient Processing and Utilization of Forest Resources, Jiangsu Provincial Key Lab for the Chemistry and Utilization of Agro-forest Biomass, College of Chemical Engineering, Nanjing Forestry University, Nanjing 210037, China

Bo Fu – Jiangsu Co-Innovation Center of Efficient Processing and Utilization of Forest Resources, Jiangsu Provincial Key Lab for the Chemistry and Utilization of Agro-forest Biomass, College of Chemical Engineering, Nanjing Forestry University, Nanjing 210037, China; orcid.org/0000-0002-0310-2075

Xinbao Zhu – Jiangsu Co-Innovation Center of Efficient Processing and Utilization of Forest Resources, Jiangsu Provincial Key Lab for the Chemistry and Utilization of Agro-forest Biomass, College of Chemical Engineering, Nanjing Forestry University, Nanjing 210037, China; orcid.org/0000-0001-7707-7362

Complete contact information is available at: <https://pubs.acs.org/doi/10.1021/acsomega.3c00693>

Notes

The authors declare no competing financial interest.

■ ACKNOWLEDGMENTS

This work was financially supported by National key research and development project (2022YFD2200802).

■ REFERENCES

(1) Wang, D.; Lai, Y. H.; Wang, P.; Leng, X. B.; Xiao, J.; Deng, L. Markovnikov Hydrosilylation of Alkynes with Tertiary Silanes

- Catalyzed by Dinuclear Cobalt Carbonyl Complexes with NHC Ligation. *J. Am. Chem. Soc.* **2021**, *143*, 12847–12856.
- (2) Du, X. Y.; Huang, Z. A. Advances in Base-Metal-Catalyzed Alkene Hydrosilylation. *ACS Catal.* **2017**, *7*, 1227–1243.
- (3) Skrodzki, M.; Patroniak, V.; Pawluc, P. Schifff Base Cobalt (II) Complex-Catalyzed Highly Markovnikov-Selective Hydrosilylation of Alkynes. *Org. Lett.* **2021**, *23*, 663–667.
- (4) Ikeuchi, T.; Hirano, K.; Uchiyama, M. Nucleophilic Activation of Hydrosilanes via a Strain-Imposing Strategy Leading to Functional Sila-aromatics. *J. Am. Chem. Soc.* **2021**, *143*, 4879–4885.
- (5) Maeda, K.; Motokura, K. Recent Advances on Heterogeneous Metal Catalysts for Hydrosilylation of Olefins. *J. Jpn. Petrol. Inst.* **2020**, *63*, 1–9.
- (6) Mukhopadhyay, T. K.; Flores, M.; Groy, T. L.; Trovitch, R. J. A Highly Active Manganese Precatalyst for the Hydrosilylation of Ketones and Esters. *J. Am. Chem. Soc.* **2014**, *136*, 882–885.
- (7) Fu, S. Y.; Zhu, M.; Zhu, T. F. Organosilicon polymer-derived ceramics: An overview. *J. Adv. Ceram.* **2019**, *8*, 457–478.
- (8) Yang, J. C.; Ma, W. S.; Hu, D. C.; Zhang, D. Q.; Wu, L.; Yang, B.; Zhang, S. H. Facile preparation and flame retardancy mechanism of cyclophosphazene derivatives for highly flame-retardant silicone rubber composites. *J. Appl. Polym. Sci.* **2021**, *138*, No. 50297.
- (9) Eckel, Z. C.; Zhou, C. Y.; Martin, J. H.; Jacobsen, A. J.; Carter, W. B.; Schaedler, T. A. Additive manufacturing of polymer-derived ceramics. *Science* **2016**, *351*, 58–62.
- (10) Meister, T. K.; Kuck, J. W.; Riener, K.; et al. Decoding catalytic activity of platinum carbene hydrosilylation catalysts. *J. Catal.* **2016**, *337*, 157–166.
- (11) Obligacion, J. V.; Chirik, P. J. Earth-abundant transition metal catalysts for alkene hydrosilylation and hydroboration. *Nat. Rev. Chem.* **2018**, *2*, 15–34.
- (12) Speier, J. L.; Webster, J. A.; Barnes, G. H. The addition of silicon hydrides to olefinic double bonds. Part II. The use of group VIII metal catalysts. *J. Am. Chem. Soc.* **1957**, *79*, 974–979.
- (13) Lewis, L. N.; Stein, J.; Colborn, R. E.; Gao, Y.; Dong, J. The chemistry of fumarate and maleate inhibitors with platinum hydrosilylation catalysts. *J. Organomet. Chem.* **1996**, *521*, 221–227.
- (14) Cui, X. J.; Junge, K.; Dai, X. C.; Kreyenschulte, C.; Pohl, M.; Wohlrab, S.; Shi, F.; Brückner, A.; Beller, M. Synthesis of single atom based heterogeneous platinum catalysts: high selectivity and activity for hydrosilylation reactions. *ACS Cent. Sci.* **2017**, *3*, 580–585.
- (15) Xie, H.; Zhang, W. X.; Hua, W. B.; Zhou, X. H.; et al. A chitosan modified Pt/SiO₂ catalyst for the synthesis of 3-poly(ethylene glycol) propyl ether-heptamethyltrisiloxane applied as agricultural synergistic agent. *Catal. Commun.* **2018**, *104*, 118–122.
- (16) Li, F. T.; Li, Y. X. Preparation of efficient and environment-friendly silica-supported EDTA platinum catalyst and its applications in hydrosilylation of olefins and methylchlorosilane. *J. Mol. Catal. A: Chem.* **2016**, *420*, 254–263.
- (17) Humayun, M.; Zada, A.; Li, Z. J.; Xie, M. Z.; Zhang, X. L.; Qu, Y.; et al. Enhanced visible-light activities of porous BiFeO₃ by coupling with nanocrystalline TiO₂ and mechanism. *Appl. Catal., B* **2016**, *180*, 219–226.
- (18) Chay, R. S.; Rocha, B. G. M.; Pombeiro, A. J. L.; Kukushkin, V. Y.; Luzyanin, K. V. Platinum Complexes with Chelating Acyclic Aminocarbene Ligands Work as Catalysts for Hydrosilylation of Alkynes. *ACS Omega* **2018**, *3*, 863–871.
- (19) Li, D. J.; Li, Q. H.; Wang, Z. R.; Ma, Z. Z.; Gu, Z. G.; Zhang, J. Interpenetrated Metal-Porphyrinic Framework for Enhanced Non-linear Optical Limiting. *J. Am. Chem. Soc.* **2021**, *143*, 17162–17169.
- (20) Bunescu, A.; Lee, S.; Li, Q.; Hartwig, J. F. Catalytic hydroxylation of polyethylenes. *ACS Cent. Sci.* **2017**, *3*, 895–903.
- (21) Williamson, J. B.; Czaplyski, W. L.; Alexanian, E. J.; Leibfarth, F. A. Regioselective C-H xanthylation as a platform for polyolefin functionalization. *Angew. Chem., Int. Ed.* **2018**, *57*, 6261–6265.
- (22) Orcajo, G.; Andrés, H. M.; Villajos, J. A.; Martos, C.; Botas, J. A.; Calleja, G. Li-Crown ether complex inclusion in MOF materials for enhanced H₂ volumetric storage capacity at room temperature. *Int. J. Hydrogen Energy* **2019**, *44*, 19285–19293.
- (23) Zhang, X.-F.; Wang, Z.; Ding, M.; Feng, Y.; Yao, J. Advances in cellulose-metal organic framework composites: preparation and applications. *J. Mater. Chem. A* **2021**, *9*, 23353–23363.
- (24) Zhang, X.-F.; Wang, Z.; Song, L.; Yao, J. In situ growth of ZIF-8 within wood channels for water pollutants removal. *Sep. Purif. Technol.* **2021**, *266*, No. 118527.
- (25) Zhang, X.; Wang, Z.; Zhong, Y.; Qiu, J. H.; Zhang, X.; Gao, Y.; Gu, X.; Yao, J. TiO₂ nanorods loaded with AuPt alloy nanoparticles for the photocatalytic oxidation of benzyl alcohol. *J. Phys. Chem. Solid* **2019**, *126*, 27–32.
- (26) Zhu, X.; Fan, Z.; Zhang, X.; Yao, J. Metal-organic frameworks decorated wood aerogels for efficient particulate matter removal. *J. Colloid Interface Sci.* **2023**, *629*, 182–188.
- (27) Song, L.; Zhang, X.; Wang, Z.; Zheng, T.; Yao, J. Fe₃O₄/polyvinyl alcohol decorated delignified wood evaporator for continuous solar steam generation. *Desalination* **2021**, *507*, No. 115024.
- (28) Zango, Z. U.; Jumbri, K.; Sambudi, N. S.; Basheer, C.; Saad, B.; et al. Removal of anthracene in water by MIL-88(Fe), NH₂-MIL-88(Fe) and mixed-MIL-88(Fe) metal-organic frameworks. *RSC Adv.* **2019**, *9*, 41490–41501.
- (29) Rahmani, E.; Rahmani, M. Catalytic process modeling and sensitivity analysis of alkylation of benzene with ethanol over MIL-101(Fe) and MIL-88(Fe). *Front. Chem. Sci. Eng.* **2020**, *14*, 1100–1111.
- (30) Kurisingal, J. F.; Rachuri, Y.; Gu, Y. J.; Choe, Y.; Park, D.-W. Fabrication of hierarchically porous MIL-88-NH₂(Fe): a highly efficient catalyst for the chemical fixation of CO₂ under ambient pressure. *Inorg. Chem. Front.* **2019**, *6*, 3613–3620.
- (31) Xie, Z. K.; Chen, W. W.; Chen, X. Y.; Zhou, X. H.; Hu, W. B.; Shu, X. G. Platinum on 2-aminoethanethiol functionalized MIL-101 as a catalyst for alkene hydrosilylation. *RSC Adv.* **2019**, *9*, 20314–20322.
- (32) Katouezadeh, E.; Zebarjad, S. M.; Janghorban, K. Morphological study of surface-modified urea-formaldehyde microcapsules using 3-aminopropyltriethoxy silane. *Polym. Bull.* **2019**, *76*, 1317–1331.
- (33) Chen, K.; Li, P.; Li, X. G.; Liao, C. G.; Li, X. G.; Zuo, Y. F. Effect of silane coupling agent on compatibility interface and properties of wheat straw/poly(lactic acid) composites. *Int. J. Biol. Macromol.* **2021**, *182*, 2108–2116.
- (34) Shimazaki, Y.; Hayasaka, S.; Koyama, T.; Nagao, D.; Kobayashi, Y.; Konno, M. A durable PtRu/C catalyst with a thin protective layer for direct methanol fuel cells. *J. Colloid Interface Sci.* **2010**, *351*, 580–583.
- (35) Zai, H.; Zhao, Y.; Chen, S.; Ge, L.; Chen, C.; Chen, Q.; Li, Y. Heterogeneously supported pseudo-single atom Pt as sustainable hydrosilylation catalyst. *Nano Res.* **2018**, *11*, 2544–2552.
- (36) Chen, Y. J.; Ji, S. F.; Sun, W. M.; Chen, W. X.; Dong, J. C.; Wen, J. F.; Zhang, J.; Li, Z.; Zheng, L. R.; Chen, C.; Peng, Q.; Wang, D. S.; Li, Y. D. Discovering partially charged single-atom Pt for enhanced antimarkovnikov alkene hydrosilylation. *J. Am. Chem. Soc.* **2018**, *140*, 7407–7410.
- (37) Hu, W. B.; Xie, H. L.; Yue, H. B.; Prinsen, P.; Luque, R. Supermicroporous silicasupported platinum catalyst for highly regioselective hydrosilylation. *Catal. Commun.* **2017**, *97*, 51–55.
- (38) Jiang, S.; Zhao, Z.; Chen, J.; Yang, Y.; Ding, C.; Yang, Y.; Wang, Y.; Wang, Y.; Liu, N.; Liu, N.; Wang, L.; Wang, L.; Zhang, X. Recent research progress and challenges of MIL-88(Fe) from synthesis to advanced oxidation process. *Surf. Interfaces* **2022**, *30*, No. 101843.
- (39) Liu, N.; Wu, J. X.; Fei, F. H.; Lei, J. Q.; Shi, W. Y.; Quan, G. X.; Zeng, S.; Zhang, X. D.; Tang, L. Ibuprofen degradation by a synergism of facet-controlled MIL-88B(Fe) and persulfate under simulated visible light. *J. Colloid Interface Sci.* **2022**, *612*, 1–12.
- (40) Safy, M. E. A.; Amin, M.; Haikal, R. R.; Elshazly, B.; Wang, J. J.; Wang, Y. M.; Wöll, C.; Alkordi, M. H. Probing the Water Stability Limits and Degradation Pathways of Metal–Organic Frameworks. *Chem.—Eur. J.* **2020**, *26*, 7109–7117.

(41) Zhang, S. P.; Zhuo, Y. F.; Ezugwu, C. I.; Wang, C.-C.; Li, C. H.; Liu, S. W. Synergetic molecular oxygen activation and catalytic oxidation of formaldehyde over defective MIL-88B(Fe) nanorods at room temperature. *Environ. Sci. Technol.* **2021**, *55*, 8341–8350.

(42) Hu, C.; Yoshida, M.; Huang, P.-H.; Tsunekawa, S.; Hou, L.-B.; Chen, C.-H.; Tung, K.-L. MIL-88B(Fe)-coated photocatalytic membrane reactor with highly stable flux and phenol removal efficiency. *Chem. Eng. J.* **2021**, *418*, No. 129469.

(43) Indulekha, K.; Rajeev, R. S.; Ninan, K. N.; Gouri, C. Polycyclic silicone polymer as novel single source precursor for the facile synthesis of nanostructured SiC. *Mater. Chem. Phys.* **2018**, *206*, 64–70.

(44) Zhang, Y. L.; Li, S. C.; Zhang, W. J.; Chen, X.; Hou, D. S.; Zhao, T. J.; Li, X. G. Preparation and mechanism of graphene oxide/isobutyltriethoxysilane composite emulsion and its effects on waterproof performance of concrete. *Constr. Build. Mater.* **2019**, *208*, 343–349.

(45) Wang, Y. Y.; Wang, Z. J.; Zhao, L.; Fan, Q. N.; Zeng, X. H.; Liu, S. L.; Pang, W. K.; He, Y.-B.; Guo, Z. P. Lithium Metal Electrode with Increased Air Stability and Robust Solid Electrolyte Interphase Realized by Silane Coupling Agent Modification. *Adv. Mater.* **2021**, *33*, No. 2008133.

(46) Wang, X.; Zhang, C.; Wu, Q. S.; Zhu, H. J.; Liu, Y. Thermal properties of metakaolin-based geopolymer modified by the silane coupling agent. *Mater. Chem. Phys.* **2021**, *267*, No. 124655.

(47) Bulushev, D. A.; Zacharska, M.; Lisitsyn, A. S.; Podyacheva, O. Y.; Hage, F. S.; Ramasse, Q. M.; Bangert, U.; Bulusheva, L. G. Single Atoms of Pt-group Metals Stabilized by N-Doped Carbon Nanofibers for Efficient Hydrogen Production from Formic Acid. *ACS Catal.* **2016**, *6*, 3442–3451.

(48) Zhu, Y.; Cao, T.; Cao, C. B.; Luo, J.; Chen, W. X.; Zheng, L.; Dong, J. C.; Zhang, J.; Han, Y. H.; Li, Z.; Chen, C.; Peng, Q.; Wang, D. S.; Li, Y. D. One-Pot Pyrolysis to N-Doped Graphene with High-Density Pt Single Atomic Sites as Heterogeneous Catalyst for Alkene Hydrosilylation. *ACS Catal.* **2018**, *8*, 10004–10011.

(49) Vakili, R.; Gibson, E. K.; Chansai, S.; Xu, S. J.; Al-Janabi, N.; Wells, P. P.; Hardacre, C.; Walton, A.; Fan, X. L. Understanding the CO Oxidation on Pt Nanoparticles Supported on MOFs by Operando XPS. *ChemCatChem* **2018**, *10*, 4238–4242.

(50) Jeelan Basha, N.; Basavarajiah, S. M.; Shyamsunder, K. Therapeutic potential of pyrrole and pyrrolidine analogs: an update. *Mol. Diversity* **2022**, *26*, 2915–2937.

(51) Meister, T. K.; Riener, K.; Gigler, P.; Stohrer, J.; Herrmann, W. A.; Kühn, F. E. Platinum Catalysis Revisited Unraveling Principles of Catalytic Olefin Hydrosilylation. *ACS Catal.* **2016**, *6*, 1274–1284.